Detectors

The telescope captures light from astronomical objects and delivers it to the focal plane where it may be detected.

The delivered image will cover the full visible/IR or radio spectrum, as transmitted by the atmosphere, but it will generally be sampled by an instrument with a filter which selects a particular wavelength range and passes that to a detector.

Silicon CCD detectors are usually used in the visible (and at X-ray/UV wavelengths on satellites).

Hybrid infrared arrays with HgCdTe or InSb layers bonded to silicon multiplexers at near-Infrared wavelengths, or doped silicon detectors e.g. Si:As at mid-infrared wavelengths.

Radio receivers use custom-built SIS chips or superconducting transition edge sensors, Kinetic Induction Devices (KIDS), bolometers etc

1

1

Semiconductors

Solid state detectors:
Photon absorption with E> band gap, promotes an electron to the conduction band.

The band gap in silicon is 1.1eV, requiring photons with λ< 1.1μm for excitation.
The bandgap can be modified by doping with impurities, such as arsenic; Si:AS bandgap ~0.05eV (λ> 25μm).

Devices are cooled to decrease the thermal population in the conduction band (reducing the dark current)

Impurities and defects affect the lattice structure

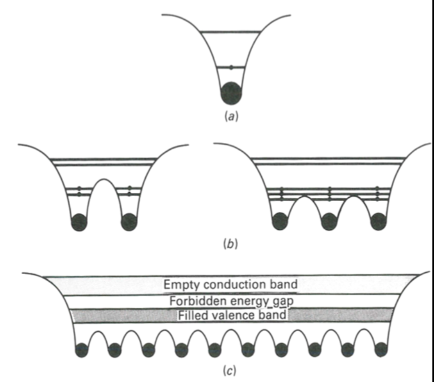

Fig. 6.3. The development of a conduction band and a valence band of electrons in a soli[d] crystalline material such as silicon.

2

2

Charge Coupled Devices

By implanting channel stops and electrodes into the silicon substrate, a set of cells can be defined within the silicon chip.

By clocking the electrodes, the charge accumulated in one cell can be moved across to the edge of the chip, where it can be read out. This is the basis of the CCD

The analogue signal is digitised by an ADC with a bias offset to ensure proper sampling

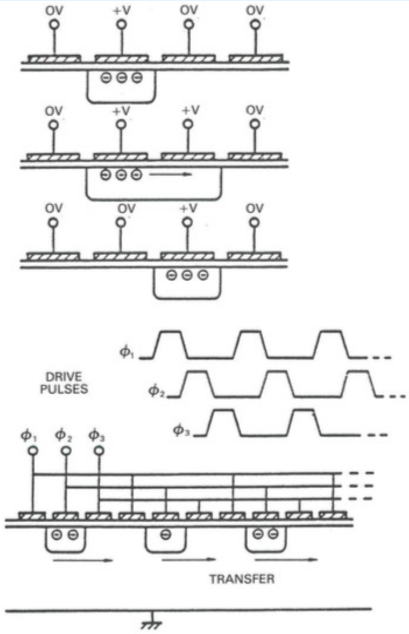

Fig. 6.9. Charge-coupling in a three-phase CCD and the associated timing waveform or clock pattern. In practice the degree of overlap between one electrode and the next depends on the CCD design. (I S McLean 1997)

3

CCD (Charge Coupled Devices)

- This simplified structure has poor charge transfer efficiency
- Charge trapping in the Si-SiO_2 interface, and surface traps caused by polishing and implantation

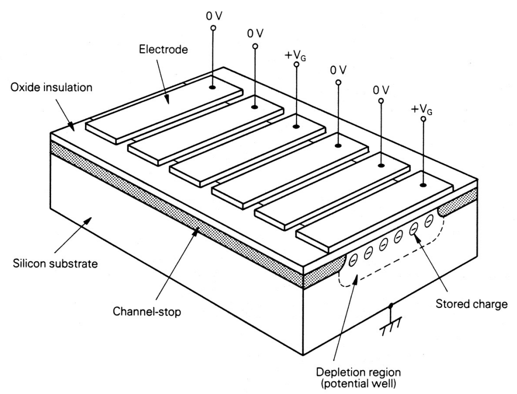

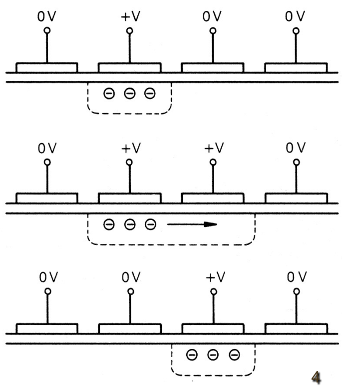

4

CCD (Charge Coupled Devices)

- Introduction of a buried-channel (n-type silicon) implant
- Charge transfer is now below the Si-SiO2 interface

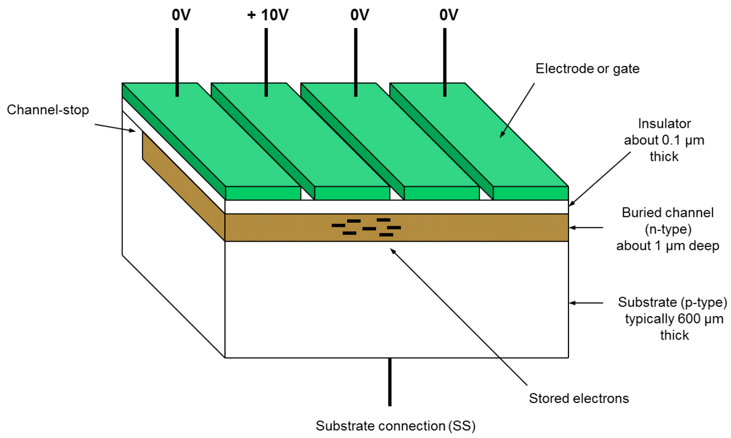

CCD pictures courtesy David Burt (e2v)

5

5

CCD Types

Full-Frame

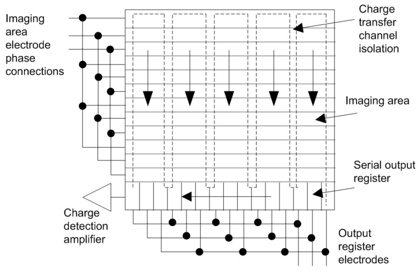

Frame-Transfer

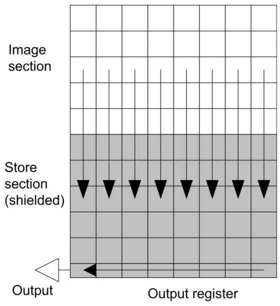

CCD read-out introduces a dead period when the detector is not integrating.

For high speed operation, can use a frame transfer device - the frame is shifted into an unilluminated part of the chip and then read out during the next exposure

6

6

Back-illumination

- Back-illumination improves Q.E. – photons not blocked by electrodes etc
- Need to thin the silicon to maintain resolution
- Add anti-reflection coating to further reduce losses
- Very thin chips have poor red response – the path through silicon is below the mean absorption depth

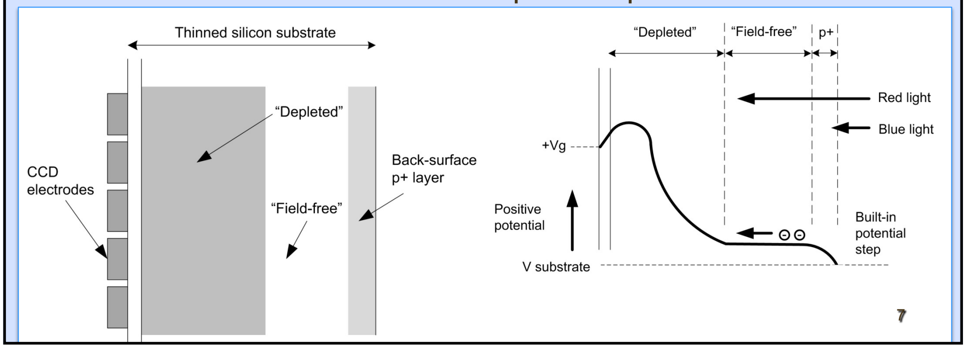

7

7

Quantum Efficiency

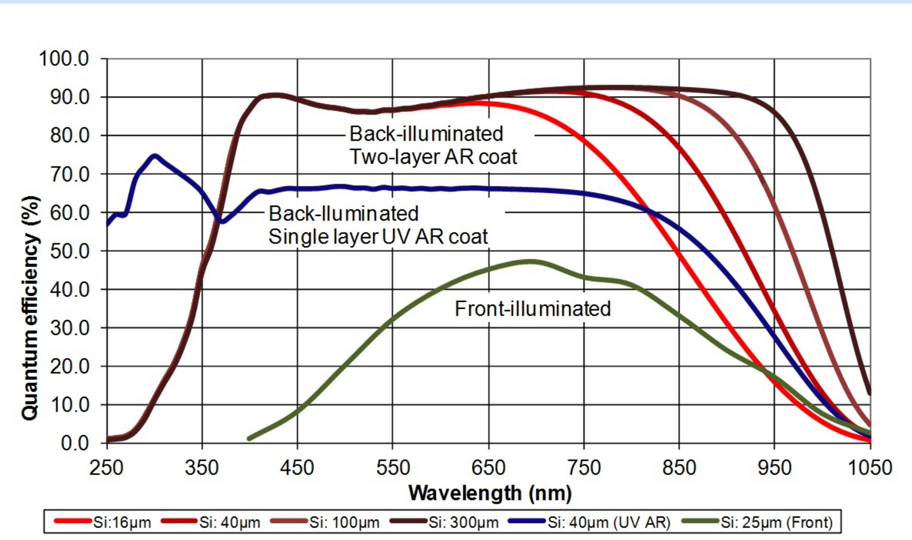

e2v technologies

8

8

Quantum Efficiency

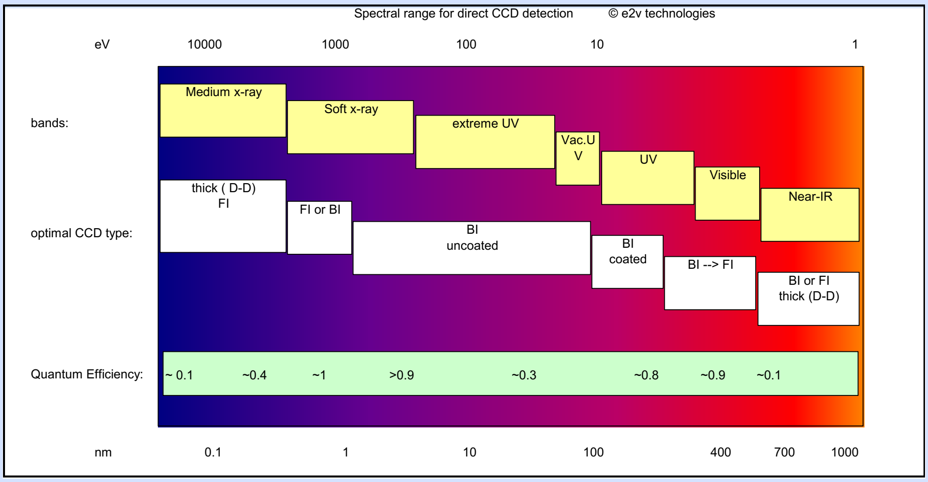

9

9

Fringing

- Interference fringing occurs at long wavelengths – internal reflections within the device, which significantly affects narrow-band imaging and spectroscopy
- Typically ≥ 750-800 nm, rising in amplitude to ≈ 20%
- Pattern is wavelength dependent
- Fringing is decreased in thicker deep depletion devices
- AR coating at the fringing wavelengths minimises internal reflections.

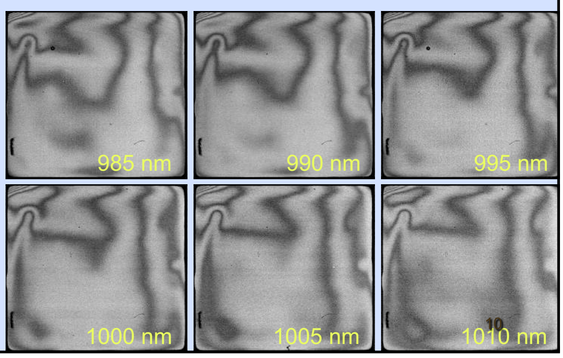

10

10

CCD Performance

• Cosmetic issues – blocked or dead columns, defects, trapping sites

•Readout noise associated with charge measurement

• Dark current due to thermal effects

• Fixed pattern noise due to geometry variations

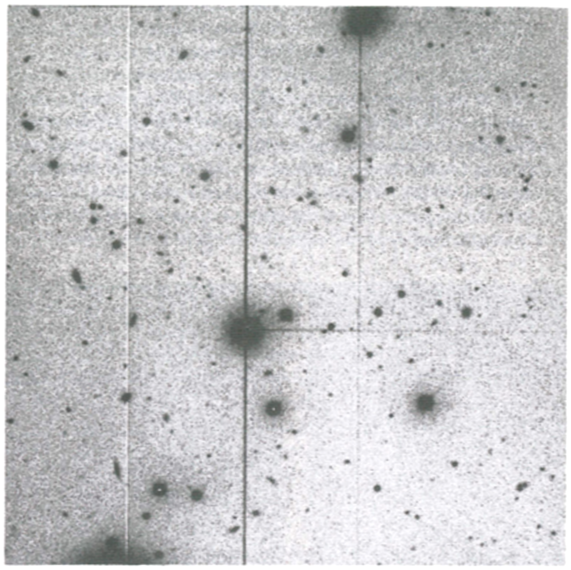

Fig. 7.8. An astronomical CCD image (displayed as a "negative") in which a bright star ha saturated in the exposure time needed to record the fainter objects. When the CCD pixel saturate it spills over and "bleeds" up and down the column. The horizontal trail is evidence of poor charg transfer efficiency in the serial register. The white line is a non-working or "dead" columr Courtesy NOAO.

11

11

Dark Current

• Leakage current from electrons having sufficient thermal energy to break free from the lattice

• Surface traps at the silicon-silicon dioxide interface are largely responsible

• Typically 1 nA cm^{-2} at 20 ºC in standard CCDs

• Thermal noise decreases by a factor of two for roughly every 7-8 ºC reduction in operating temperature

• ≈ 2 electrons/pixel/hour at -100 ºC (10 µm pixel)

• CCDs typically operated at 77 K (LN2) to 150 K

• Dark current has associated shot noise and a relative statistical pixel-to-pixel non-uniformity of ~ 3-10 % RMS

12

12

Fixed Pattern Noise

•Fixed Pattern Noise : Variations in pixel responsivity due to geometry variations

- Typically in the range 1-2 % for a good CCD
- Removal by 'flat-fielding'
- An exposure of a uniform field to remove local pixel-to-pixel sensitivity variations – some are intrinsic other may arise from dust on filters or other optics
- Global flat-field (often generated from twilight exposures) to remove large scale variations across the chip

13

13

CCD Dynamic Range

- Depends on full-well capacity and readout noise
- Linearity generally very good – 0.1% to >80% full well
- Well capacity driven by pixel design and size

  For a 12 × 12 μm pixel ≈ 100,000 e to 200,000 e

Readout noise is a function of readout rate

≈ 2 electrons RMS at 100 kHz, ≈ 5 electrons RMS at 1 MHz

- Instantaneous pixel dynamic range

  Could well be ≈ 100,000 (> 16 bits)

- e2v CCD231

  15 × 15 μm 4-phase pixel full-well capacity = 350,000 e

- And…

  24 × 24 μm 4-phase pixel can store 10^6 electrons!

14

14

Signal-to-Noise Ratio (SNR)

- Photon distribution obeys Poisson statistics (shot noise)
- Noise sources:
- Photon noise from **S**ource
- Photon noise from **B**ackground
- Photon-equivalent noise from detector **D**ark current
- **R**ead noise of detector

$$SNR = \frac{S \cdot t}{\sqrt{(S+B+D)t+R^2}} = \frac{S \cdot \sqrt{t}}{\sqrt{(S+B+D)+R^2/t}}$$

Note: S and B in electrons, includes Q.E.

- Aim to be limited by the Background photon flux (unless the target is very bright) rather than by the detector noise

15

15

CCD Specification

e2v CCD231

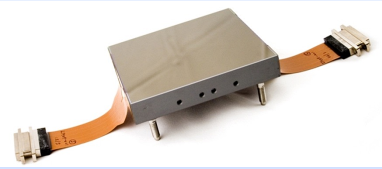

SUMMARY PERFORMANCE (Typical)

Number of pixels	6144(H) x 6160(V)
Pixel size	15 µm square
Image area	92.2 mm x 92.4 mm
Outputs	4
Package size	98.5 x 93.7 mm
Package format	Silicon carbide with two flexi connectors
Focal plane height, above base	20.0 mm
Height tolerance	±15 µm
Connectors	Two 37-way micro-D
Flatness	<40 µm (peak to valley)
Amplifier sensitivity	7 µV/e$^-$
Readout noise	5 e$^-$ at 1 MHz 2 e$^-$ at 50 kHz
Maximum pixel data rate	3 MHz
Charge storage (pixel full well)	350,000 e$^-$
Dark signal	3 e$^-$/pixel/hour (at –100 °C)

16

16

Cosmic Rays

•Cosmic rays (or other energetic particles) can liberate a large number of electrons from the atoms hit

• Can be limited to single pixels - head-on strikes –or short or long track - glancing strikes

• Signal produced generally much bigger than from an astronomical target. Usually make several shorter exposures so that pixels suffering Cosmic Ray hits are only affected in a subset of the data.

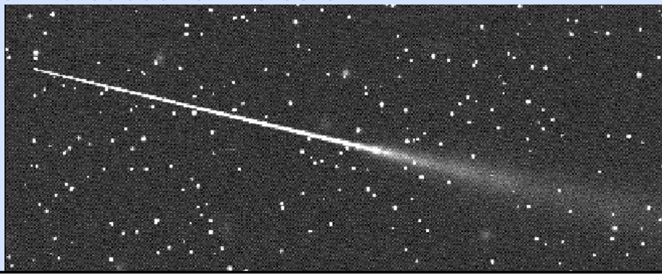

17

17

Image Retention or Persistence

• Image retention after saturation

• Charge gets trapped in the Si-SiO2 interface

• Long (many minutes) and temperature dependent release time

• Region of enhances signal or higher dark current at locations with high illumination levels

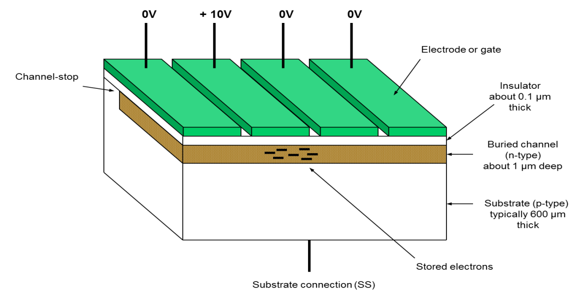

CCD pictures courtesy David Burt (e2v)

18

18

Buttable CCDS : Large Focal Planes

63 CM Diameter Focal Plane with 3.2 GigaPixels

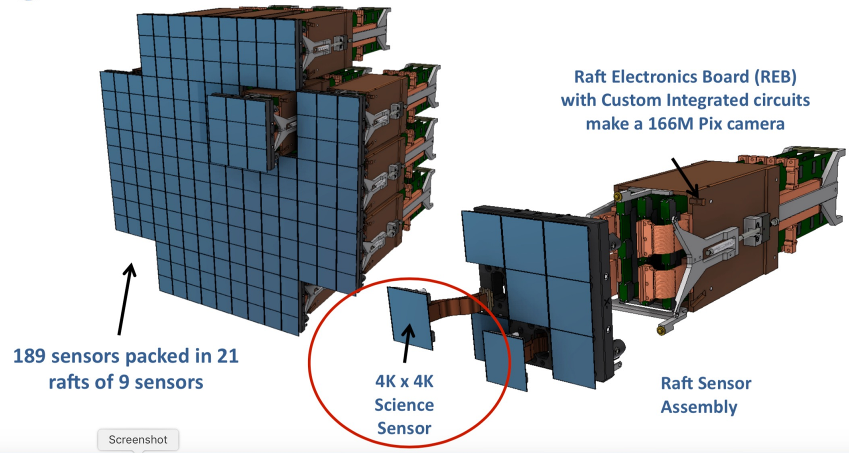

19

Completed 3.2 gigapixel LSST Camera

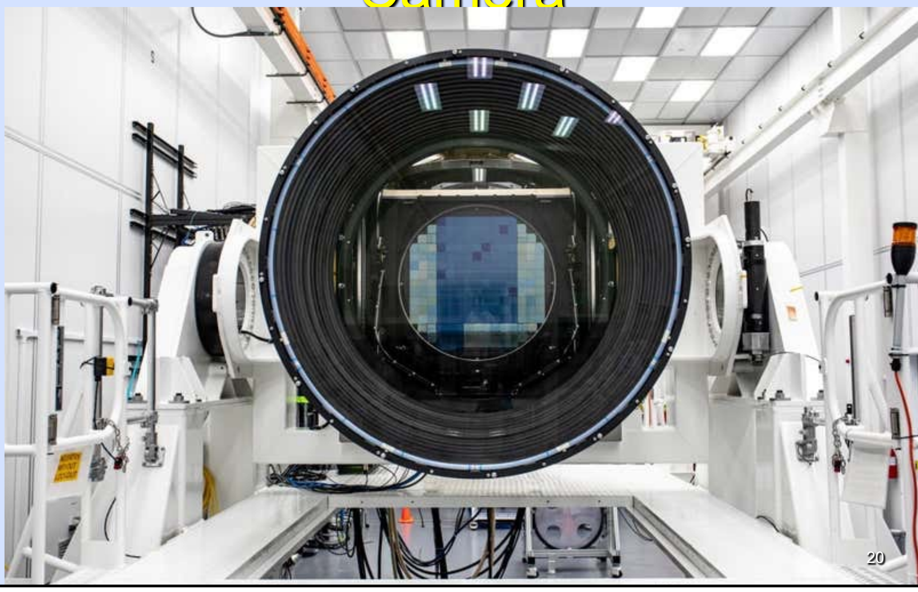

20

CMOS Sensors

- A new(ish) type of image sensor fabricated in CMOS
- Silicon chip technology used in microprocessor systems
- Allows the integration of a large array of pixels alongside all of the electronics needed to address the array, buffer the analogue video signal and even digitise it

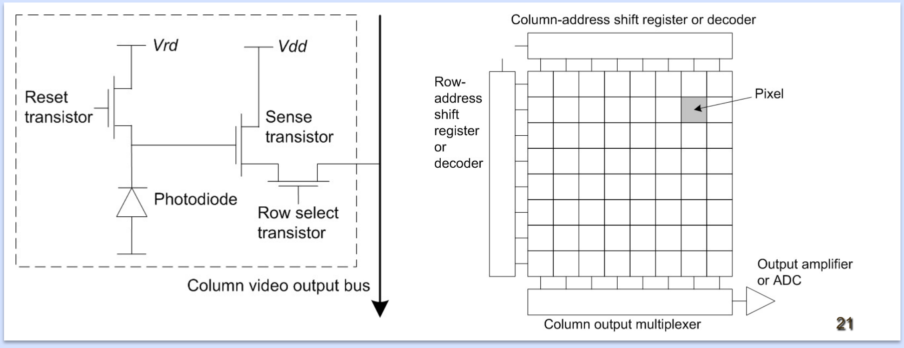

21

21

IR Sensors

- Broadly split into Photo-conductors and Bolometers
- NIR using intrinsic semi-conductors with smaller band-gaps such as HgCdTe or InSb in formats up to 4k x 4k pixels.
- HgCdTe operated at ~77K, InSb at ~40K
- MIR using BIB (blocked impurity band) to get high doping with low dark current – formats up to 1k x 1k. Si:As operated at ~7K
- FIR using extrinsic (doped) semi-conductors with added impurities

22

22

HgCdTe IR Sensors

- Mercury Cadmium Telluride - three key technologies:
  - Growth and processing of the HgCdTe detector layer
  - Design and fabrication of the CMOS ROIC
  - Hybridization of the detector layer to the CMOS ROIC

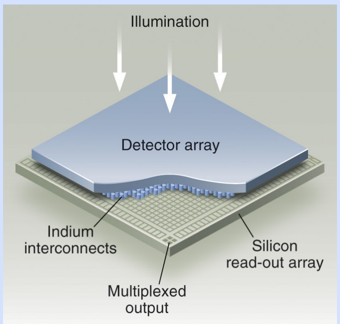

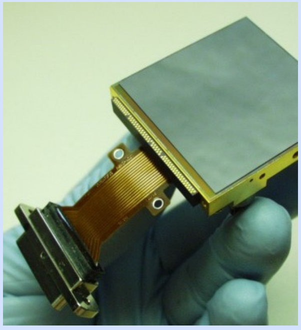

23

23

HgCdTe IR Sensors

- Bandgap can be "tuned" from 0.1 eV to 1.5 eV by varying the mixture of Hg and Cd
- Near-IR ≈ 1.7, 2.5 μm cutoff - defined as 50 % of peak QE
- Mid-wave IR ≈ 5 μm
- long-wave IR ≈ 10 μm
- Up to ≈ 15 μm is theoretically possible
- Best detectors are grown by MBE (Molecular Beam Epitaxy)
- HgCdTe grown on CdZnTe substrate
- Teledyne (formerly Rockwell Scientific) sensors are most widely used in astronomy, though the biggest IR camera uses 16 Raytheon 2k x 2k detectors on VISTA (P.I. Gavin Dalton)

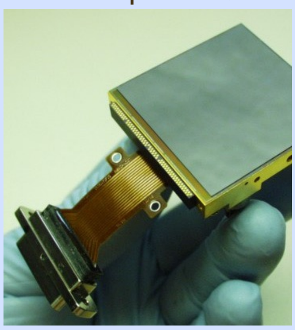

24

24

Performance

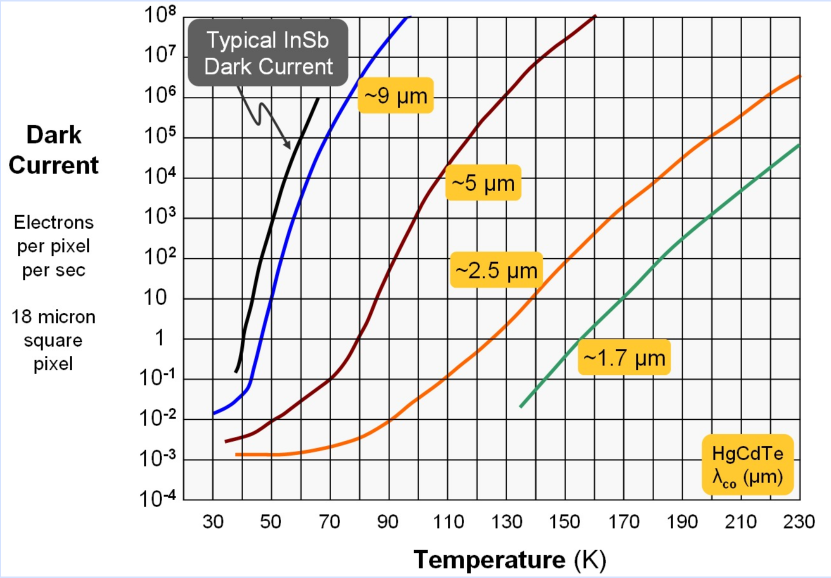

Lower temperature decreases dark current, but may also decrease QE 25

25

HgCdTe Response

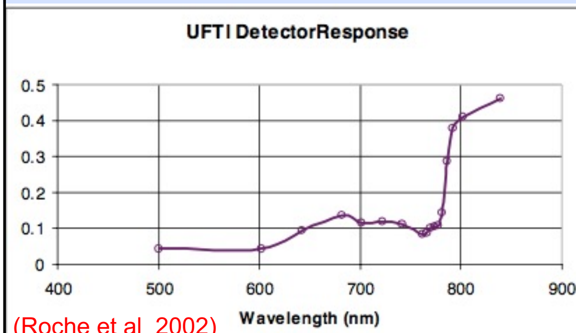

(Roche et al 2002)

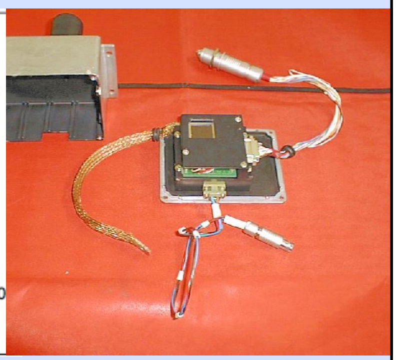

UFTI detector – Hawaii-I 1028 x 1028 Rockwell device
Near-IR camera on UKIRT with a fine (0.09 arcsec) pixel scale

Short wave cut off at 0.78um but with residual sensitivity to 0.5um.
Dark current <1 e-/pix/min at 80 K
Read noise ~10e- with multiple NDR, 26e- with CDS, ~99.7% operable pixels

Hawaii-2RG (H2RG), 2K × 2K array with 18 µm pixel pitch, sensitive to 2.5um, QE~ 80-90%. 26

26

HgCdTe Readout

• Source-follower is the same as CCD/CMOS and subject to reset noise and removal by CDS

• Directly addressable pixels (rather than charge transfer in CCD) allows multiple, non-destructive reads to reduce Read noise

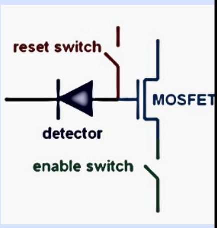

• Output amplifier noise 15 - 50e^- , full-well ≈ 10^5 to 10^6 e^-

• Noise reduction by:

• Averaging multiple samples at beginning and end of integration (Fowler & Gatley 1990). 4 reset samples and 4 signal samples reduces noise by √n =2

• Or can perform continuous sampling during integration 'up the ramp' (R Glendinning et al 1990)

27

27

HgCdTe Readout

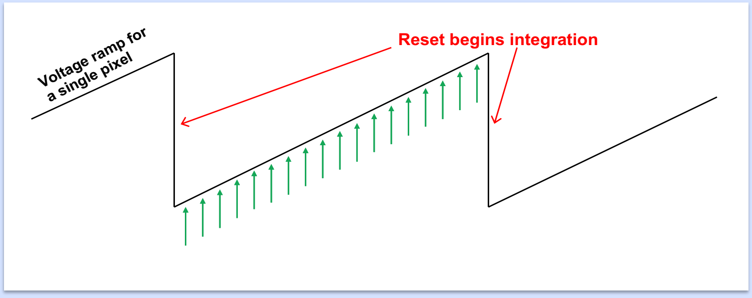

•Directly addressable pixels (rather than charge transfer in CCD) allows multiple, non-destructive reads to reduce Read Noise

• Output amplifier noise 15 - 50e^- , full-well ≈ 10^5 to 10^6 e^-

• Noise reduction by:

• Averaging multiple samples at beginning and end of integration (Fowler & Gatley 1990). 4 reset samples and 4 signal samples reduces noise by √n =2

• Or continuously sample during (R Glendinning et al 1990)

28

28

IR Sensors Issues

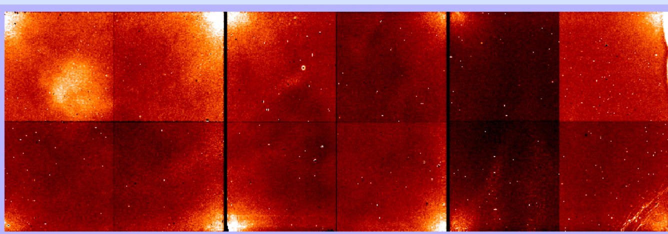

Dark Current

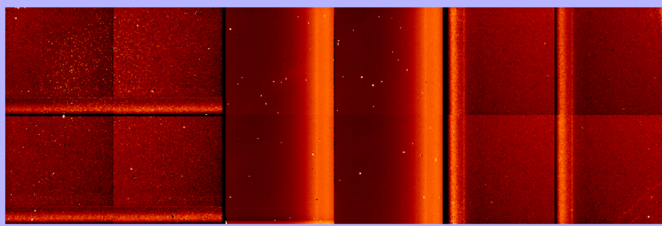

Spatially-dependent bias ("shading")

29

29

IR Sensors Issues

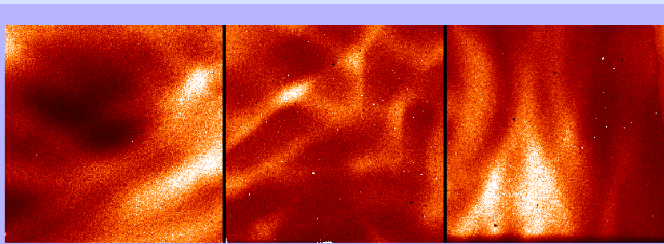

QE Spatial Variations

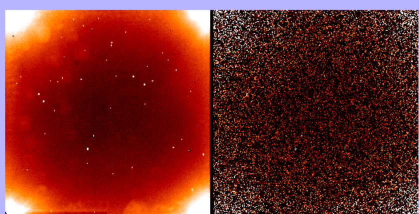

signal resulting noise

Amplifier (MUX) Glow

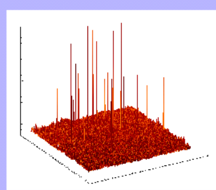

Bad Pixels

30

30

IR Sensors Issues

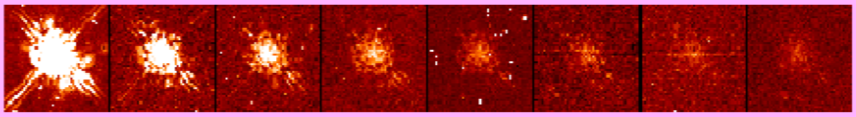

Latent Images ("persistence")

Bright objects can leave residual charge after pixel reset which appears as a 'ghost' in subsequent exposures.
The remnant typically fades after a minute or two.
To minimise the impact,
Avoid looking at faint things immediately after bright things, or at least not in the same part of the chip

31

31

Other Sensors

Intrinsic

- **InSb** **Indium Antimonide 5.6 µm cut-off λ at 77 K used in instruments that cover JHKLM bands**

Extrinsic BIB (Blocked Impurity Band)

- **Si:As** **Silicon Arsenide 5-28 µm**
- **Si:Sb** **Silicon Antimonide 7-40 µm**

At thermal IR wavelengths, 3-30 µm, the large photon flux from the telescope and sky background requires rapid array read-out to avoid saturation. Higher dark currents can be tolerated in these conditions, as the detector is operated near full well capacity; frame times may be ~10 msec.

32

32

Si:As BIB detector array

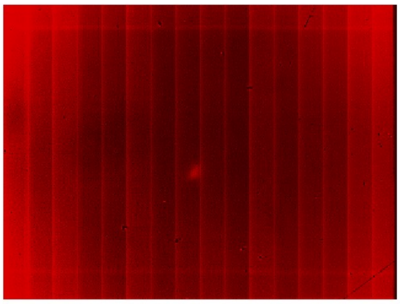

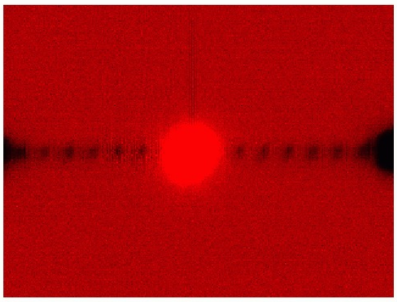

- Multi-channel readouts for fast frame rates, but they can suffer from discontinuities and cross-talk. 16 readout channels in this 320x240 Si:As Teledyne array
- Left: raw frame of a bright star obtained with TReCS/Gemini
- Right: image after chop & nod subtraction showing crosstalk

33

Incoherent Long Wavelength Detectors

At microwave and radio frequencies, the photon energy is <1meV corresponding to sub-K temperatures.

Bolometers : germanium thermistors of low thermal inertia, heat up on absorption of radiation.

Individual devices coupled with waveguides to telescope.

Operated at mK temperatures but even then may not be background-limited

Labour intensive production – limited pixel numbers, individual wiring and read-out

SCUBA individual pixel

SCUBA focal plane

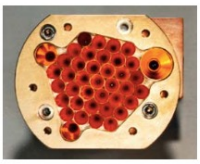

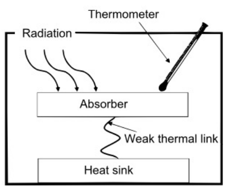

Figure 1: Schematic of a bolometer. Radiation is absorbed in the absorber. A thermometer detects the resulting increase in temperature. Heat is removed by a weak thermal link to a heat sink.

34

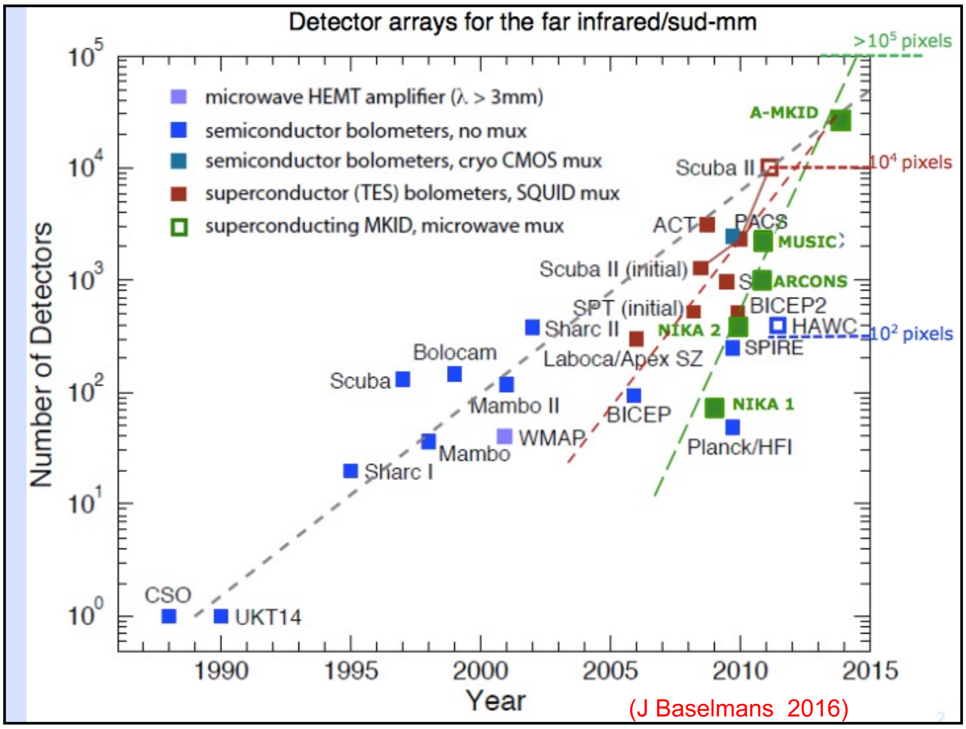

35

Array Detectors : TES

- Transition edge sensor devices exploit the super-conducting transition to give high sensitivity (large dR/dT)
- TES arrays are bump-bonded to a multiplexor allowing large format arrays
- Operated at ~60mK, with bias level control to keep on transition
- Instrument cooled below 10K to reduce background
- SCUBA-2 maps the sky at 450 and 850um with 4 arrays each with 1280 TES pixels in each waveband.

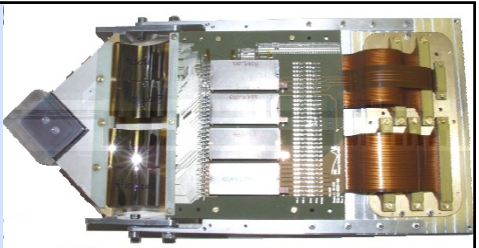

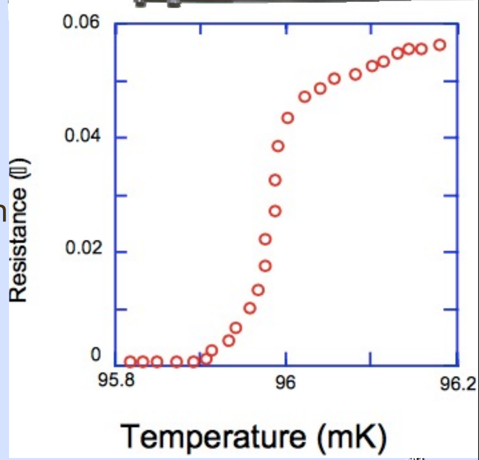

(A Woodcraft 2006)

36

Kinetic Induction Devices

KIDS use superconductor *below* the transition temperature

Radiation breaks Cooper pairs which act rather like electron-hole pair creation in semiconductor, but with smaller energy gap

Signal detection is via the change in AC inductance, which should lead to simpler detector fabrication and signal processing

Instrument will still need to be cooled below 10K, and the detectors to be maintained near 50mK

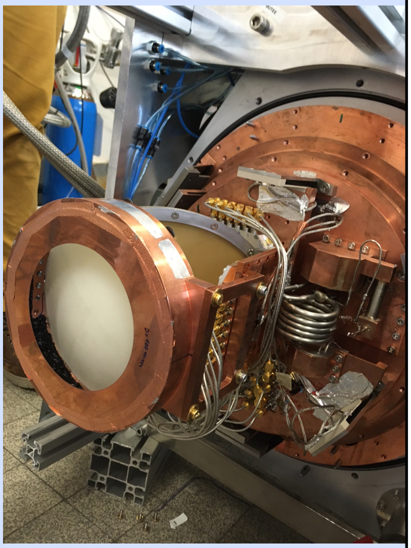

Concerto instrument mounted on APEX. Operates at 120-300 GHz with 2 x 2152 pixels

37

37

Kinetic Induction devices

- Promising technology for large format, microwave detector arrays
- Pixels can provide low energy-resolving imaging systems
- Potential at other wavelengths, including Near-IR/visible

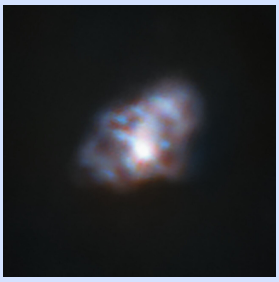

Crab nebula imaged with Concerto

NGC6334 imaged with Concerto

38

38

Coherent Detector Systems

- Single or few pixel receivers sensitive to both intensity and phase are used for spectroscopy or in interferometers
- At high frequencies, generally Superconductor-Insulator-Superconductor (SIS) devices The incoming electromagnetic wave can excite a charge carrier sufficiently for quantum tunneling across the bandgap to occur.

ALMA operates at frequencies too high for direct amplification. Mixing with a stable wave from a Local Oscillator gives a beat pattern that can be processed

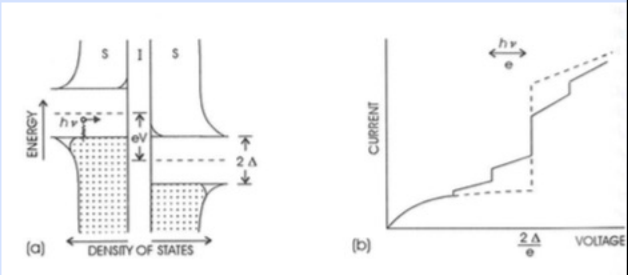

Fig. 12.15. (a) shows the basic structure of the energy levels in an SIS detector. No current flows if $eV < 2\Delta$. Absorption of a photon can excite a charge carrier to the energy where the tunnel effect occurs; (b) shows the current–voltage behaviour without illumination (solid line) and with photons present (dashed line).

39

Synoptic diagram of heterodyne receivers (basic building blocks)

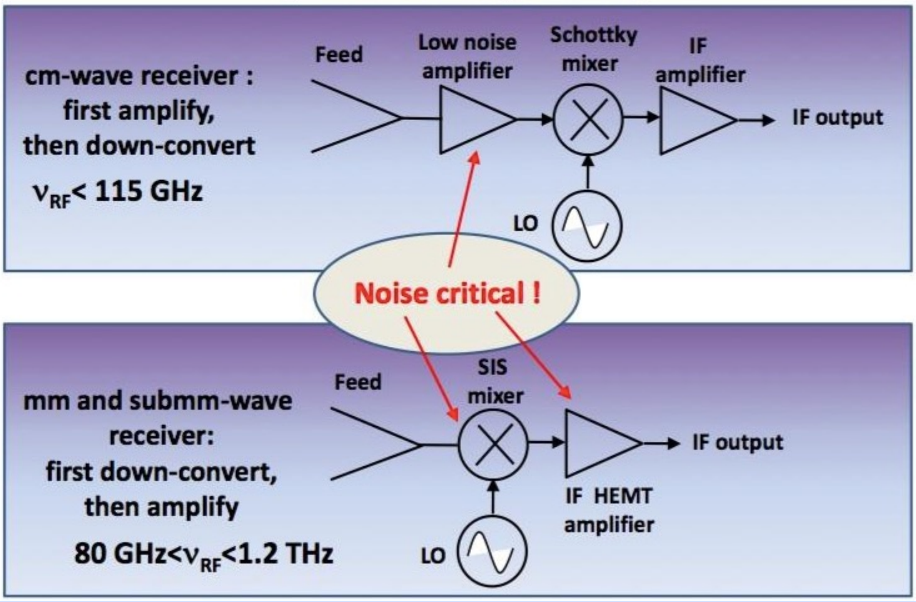

40

Heterodyne Signal Processing

- At high frequencies, need a multi-stage process: e.g
  - ALMA Band 9 (602-720 GHz) is mixed with a stable oscillation between 610-712 GHz to give an IF between 4-12GHz.
  - This Intermediate Frequency is passed to a second mixing stage with LO2 ~4-10GHz to give IF(2) ~ 0-2GHz which can be transmitted to the correlator

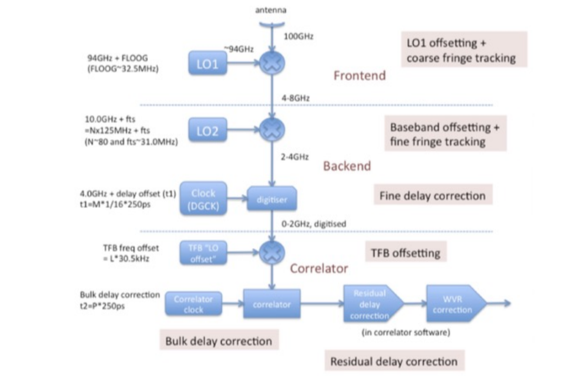

Figure B.1: Overview of ALMA frequency downconversion, LO mixing and delay corrections. This takes place in the Frontend, Backend, and Correlator. Example frequencies are given for an observation at a sky frequency of 100 GHz seen in the USB. Some LOs (e.g. LO1) are continuously tunable; others have quantized tuning steps, such as LO2 (which can be changed in a multiple ("N") of 125 MHz plus an finely-adjustable offset of "fts"), the TFB LO (which uses a multiple "L" of 30.5 kHz) and the Bulk Delay Correction (which has steps of 250 ps,

TFB Tunable Fillter Bank

41

41

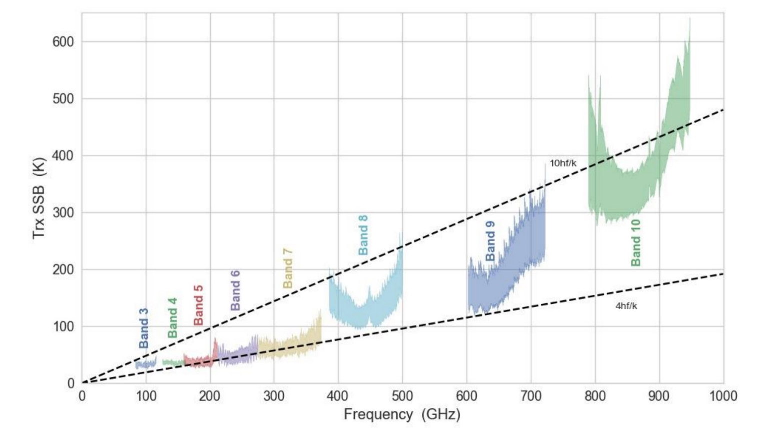

Figure 1: Receiver noise temperature for the ALMA receiver, where the shaded region encompasses 75% of the receivers about the median receiver temperature. Bands 3-8 are 2SB receivers, and Bands 9 and 10 are DSB. The noise temperature shown for the DSB receivers are twice the DSB temperatures. Band 1, which is under construction, has a receiver specification of < 25 K across 80% of the band.

- *Noise temperatures for the ALMA Receiver Bands plotted against receiver frequency on the horizontal axis. The low frequency receiver bands 4 – 7 have a performance within a factor 4 of the quantum limit. Gains can come from wider bandwidths or efficiency improvements, especially low-noise, wide-band amplifiers.*
- *Band 1 (35 – 50 GHz) are being deployed and Band 2 receivers are in production.* 42

42

Other Detectors and Developments

- Photomultiplier tubes – used in CTA
  - Fast response, blue/UV sensitivity
- Avalanche photo-diodes (APDs)
  - High sensitivity, low noise, useful for Wavefront Sensors and fringe tracking
  - HgCdTe APDs from Selex have demonstrated sub-electron read noise (G Finger et al 2012)
- Detector developments:
  - CCDs & IR hybrids :Larger formats, better uniformity, lower noise
  - CMOS developments
- Microwave & Radio : wider bandwidths, lower noise

43

43

References

- Basic Image Processing and CCD features :
- https://www.eso.org/~ohainaut/ccd/
- Starlink CCD Data Reduction Cookbook :
- http://www.starlink.ac.uk/docs/sc5.htx/sc5.html
- "Infrared Detector Arrays for Astronomy" - G.H. Reike, Annual Review of Astronomy and Astrophysics, 2007
- ALMA Technical Handbook
- https://almascience.eso.org/documents-and-tools/cycle9/alma-technical-handbook

44

44